Computational Fluid Dynamics Simulation of the Solid Suspension in a Stirred Slurry Reactor

A. R. Khopkar,[†] G. R. Kasat,[‡] A. B. Pandit,[‡] and V. V. Ranade*,[†]

Industrial Flow Modeling Group, National Chemical Laboratory, Pune, India 411 008, and Chemical Engineering Department, University Institute of Chemical Technology, Mumbai, India 400 019

A comprehensive computational fluid dynamics CFD model was developed in the present study to gain insight into the solid suspension in a stirred slurry reactor. The preliminary simulations highlighted the need for the correct modeling of the interphase drag force. A two-dimensional model problem was then developed using CFD to understand the influence of free stream turbulence on the particle drag coefficient. The proposed correlation was then incorporated in a two-fluid model (Euler−Euler) along with the standard $k-\epsilon$ turbulence model with mixture properties to simulate the turbulent solid−liquid flow in a stirred reactor. A multiple reference frame approach was used to simulate the impeller rotation in a fully baffled reactor. A computational model was mapped on to a commercial CFD solver FLUENT6.2 (of Fluent Inc., USA). The model predictions were compared with the published experimental data of Yamazaki et al. [*Powder Technol.* **1986**, *48*, 205] and Godfrey and Zhu [*AIChE Symp. Ser.* **1994**, *299*, 181]. The predicted results show reasonably good agreement with the experimental data. The computational model and results discussed in this work would be useful for extending the applications of CFD models for simulating large stirred slurry reactors.

1. Introduction

In the chemical process industry, catalytic reactions are usually carried out in a stirred reactor. In such reactors, the knowledge of the solid catalyst concentration distribution over the reactor (suspension quality) is an important parameter required for reliable design, optimum performance, and scale-up of the reactors. Despite significant research efforts, prediction of design parameters to ensure an adequate solid suspension is still an open problem for design engineers. Design of stirred slurry reactors relies on empirical correlations obtained from the experimental data. These correlations are prone to great uncertainty as one departs from the limited database that supports them. Moreover, for higher values of solid concentration, very few experimental data on local solid concentration is available because of the difficulties in the measurement techniques. Considering this, it would be most useful to develop computational models, which will allow "a priori" estimation of the solid concentration over the reactor volume.

A brief review of recent literature shows substantial progress in simulating flow in a stirred reactor using computational fluid dynamics (CFD). CFD models were shown to be successful in simulating single-phase flow generated by impeller(s) of any shape in complex reactors.[3] For multiphase flows, the complexity of modeling increases considerably and this remains an area for further research and development. Despite the complexity, several attempts have been made to simulate the solid−liquid flow in stirred reactors. Most of these studies are focused on predicting the solid concentration distribution in the stirred reactors. Although some degree of success is reported, a number of limitations are apparent.

Earlier studies have used the simulated single-phase flow field of continuous phase to simulate the solid suspension in the reactor.[4−6] All these studies assumed one-way coupling between both the phases. The mass balance equation over each control volume was solved to calculate the solid holdup/concentration profiles. The assumption of using a one-way coupling to simulate solid suspension limits the application of the proposed model for simulating solid suspensions with lower solid loading ($\leq$5%). Decker and Sommerfeld[7] and Barrue et al.[8] have performed two-way coupled simulations using the Euler−Lagrange approach. However, the simulations with the Euler−Lagrange approach can only handle slurries with a low solid volume fraction ($\leq$5%) and hence cannot be used for concentrated slurries. There are few published studies which have reported the simulation of the solid suspension in a stirred reactor using a two-fluid model.[9−16] They have predicted the suspension quality with reasonable success, but all these studies were limited to a low volume fraction of solids ($\leq$5%). However, stirred reactors with a solid volume fraction more than 10% are commonly encountered in some industrial applications. Recently, Barrue et al.[17] have simulated the solid suspension in a stirred reactor with 26% of the solid volume fraction. Although the predicted solid distribution showed reasonable agreement with the experimental data, experimental measurements were used to supply the boundary conditions for the CFD model. Oshinowo and Bakker[18] numerically studied the suspension of solids in a stirred reactor equipped with the single as well as multiple impeller system. They have used the Eulerian granular multiphase (EGM) model with four-way coupling within and between the phases. The comparison of the predicted results with the experimental data showed reasonably good agreement. Oshinowo and Bakker,[18] however, carried out simulations with a rather smaller number of computational cells (around 100 000 cells). An adequate grid resolution (usually around 300 000 cells) is, however, essential to correctly simulate flow around impeller blades and to predict the turbulent quantities adequately.[19]

Apart from the simulation of the suspension quality, the published studies also highlighted the influence of free stream turbulence on the interphase drag force formulation.[9,20−23] Interphase drag force was found to affect the distribution of solid holdup. Though a few correlations are available[20−23] to estimate the turbulence correction term, a few limitations are

* To whom correspondence should be addressed. E-mail: vv.ranade@ncl.res.in.

[†] National Chemical Laboratory.

[‡] University Institute of Chemical Technology.

10.1021/ie050941q CCC: $33.50
Published on Web 05/12/2006

still apparent. The experimental data used to formulate these correlations was measured with very low solid holdup ($\alpha \approx 1\%$). The performance of these correction terms with high solid loading ($\alpha > 5\%$) is not yet known. No information is available on the influence of solid holdup or particle Reynolds number on the proposed correction to account for prevailing turbulence. Considering the limitations in the published studies, the present work has been undertaken to systematically study the influence of different interphase drag force formulations on the predicted suspension quality for a dense solid−liquid system.

In the present work, the solid suspension in a fully baffled reactor was simulated. The two-fluid model based on the Eulerian−Eulerian approach along with a standard $k-\epsilon$ turbulence model with mixture properties was used. A multiple reference frame (MRF) approach was used to model the impeller rotation. The computational model developed in this work was used to simulate solid−liquid flow in the experimental setup used by Yamazaki et al.[1] and Godfrey and Zhu.[2] The model predictions were evaluated by comparing predictions with the experimental data.

2. Mathematical Modeling

2.1. Model Equations. Most of the applications involving solid−liquid flows in a stirred reactor are in the turbulent regime. Therefore, the Reynolds averaged mass and momentum balance equations for each phase in the turbulent flow regime were written as (without considering mass transfer)

$$\frac{\partial(\alpha_q\rho_q)}{\partial t} + \nabla\cdot(\alpha_q\rho_q\vec{U}_{q,i} - \rho_q D_{12}\nabla\alpha_q) = 0 \qquad (1)$$

$$\frac{\partial(\alpha_q\rho_q\vec{U}_{q,i})}{\partial t} + \nabla\cdot(\alpha_q\rho_q\vec{U}_{q,i}\times\vec{U}_{q,i}) = -\alpha_q\nabla\vec{p} - \nabla\cdot(\alpha_q\bar{\bar{\tau}}_{q,ij}^{(\mathrm{lam})}) - \nabla\cdot(\alpha_q\bar{\bar{\tau}}_{q,ij}^{(\mathrm{t})}) + \alpha_q\rho_q g_i + \vec{F}_{12,i} \qquad (2)$$

Here, $q = 1$ and $q = 2$ denote the continuous phase (liquid) and the suspended phase (solid), respectively, and i is the direction. $\vec{U}_q$ and α_q are the time-averaged values of the velocity and volume fraction of phase q, respectively. It should be noted that the time-averaged pressure, $\vec{p}$, is shared by both of the phases and, therefore, appears in the governing equations of all the phases. The term ρ_q is the density of the phase q, and D_{12} is the turbulent diffusivity of the dispersed phase. $F_{12,i}$ is the time-averaged interphase force in the i direction and is discussed later in this section. Here, $\alpha_q\rho_q g_i$ is the external body force on the phase q. Also, $\bar{\tau}_{q,ij}^{(\mathrm{lam})}$ is the stress tensor in the phase q due to the viscosity and $\bar{\tau}_{q,ij}^{(\mathrm{t})}$ is the Reynolds stress tensor of phase q (representing contributions of correlation of fluctuating velocities in momentum transfer). In this work, we used Boussinesq's eddy viscosity hypothesis to relate the Reynolds stresses with gradients of time-averaged velocity as

$$\bar{\bar{\tau}}_{q,ij}^{(\mathrm{t})} = \mu_{\mathrm{t}q}\left((\nabla\vec{U}_{q,i} + (\nabla\vec{U}_{q,i})^{\mathrm{T}}) - \frac{2}{3}I(\nabla\vec{U}_{q,i})\right) \qquad (3)$$

Here, $\mu_{\mathrm{t}q}$ is the turbulent viscosity of the phase q and I is the unit tensor. Different turbulence models are available in the literature for estimating the turbulent viscosity. In most of the published studies, the standard $k-\epsilon$ turbulence model (with mixture or with dispersed formulation) was used for the estimation of the turbulent viscosity. The standard $k-\epsilon$ turbulence model does not predict the turbulent quantities accurately for rotating flows. Recently, Derksen[16] has used large eddy simulations (LES) to simulate the solid suspension in stirred tanks. Such simulations, however, still require a significant amount of CPU time and therefore are not yet fine-tuned for fast process design. Also, such simulations have not yet been validated for the higher solid concentrations of the slurries. Recently, Montante and Magelli[24] have concluded that the standard $k-\epsilon$ turbulence model with mixture properties gives a qualitatively fair representation of the solid distribution in stirred slurry reactors. Following their recommendations, we have therefore used the standard $k-\epsilon$ turbulence model with mixture properties to estimate the turbulent viscosity of the mixture. The governing equations for the turbulent kinetic energy, k, and the turbulent energy dissipation rate, ϵ, were solved using mixture properties and are listed below:

$$\frac{\partial}{\partial t}(\rho_{\mathrm{m}}\phi) + \nabla\cdot(\rho_{\mathrm{m}}\vec{U}_{\mathrm{m},i}\phi) = -\nabla\cdot\left(\frac{\mu_{\mathrm{tm}}}{\sigma_{\phi\mathrm{m}}}\nabla\phi\right) + S_\phi \qquad (4)$$

where ϕ can be the turbulent kinetic energy or the turbulent energy dissipation rate for the mixture. The symbol σ_ϕ denotes the turbulent Prandtl number for variable ϕ. S_ϕ is the corresponding source term for ϕ of the mixture. Source terms for the turbulent kinetic energy and dissipation can be written as

$$S_k = G - \rho_{\mathrm{m}}\epsilon S_\epsilon = \frac{\epsilon}{k}[C_1 G - C_2\rho_{\mathrm{m}}\epsilon] \qquad (5)$$

where G is the generation of turbulence in the mixture. Turbulence generation due to mean velocity gradients, G, and μ_{tm}, the turbulent viscosity for the mixture, were calculated as

$$G = \frac{1}{2}\mu_{\mathrm{tm}}(\nabla\vec{U}_{\mathrm{m},i} + (\nabla\vec{U}_{\mathrm{m},i})^{\mathrm{T}})^2 \quad \mu_{\mathrm{tm}} = \frac{\rho_{\mathrm{m}}C_{\varpi}k^2}{\epsilon} \qquad (6)$$

where,

$$\rho_{\mathrm{m}} = \sum_{q=1}^{n}\alpha_q\rho_q \quad \vec{U}_{\mathrm{m}} = \frac{\sum_{q=1}^{n}\alpha_q\rho_q\vec{U}_q}{\sum_{q=1}^{n}\alpha_q\rho_q} \qquad (7)$$

Standard values of the $k-\epsilon$ model parameters were used in the present simulations ($C_1 = 1.44$, $C_2 = 1.92$, $C_{\varpi} = 0.09$, $\sigma_k = 1.0$, and $\sigma_\epsilon = 1.3$).

In the Reynolds averaging procedure, the turbulent dispersion of the dispersed/ suspended phase was modeled using the turbulent diffusivity, D_{12}, in the mass balance equation (eq 1). It should be noted that the contribution of turbulent dispersion force is significant only when the size of the turbulent eddies are larger than the particle size. In the case of a solid−liquid stirred reactor, even for the laboratory scale, the ratio of the largest energy containing eddy (in millimeters) and the particle size was found to be around 10. Therefore, the contribution of the turbulent dispersion is likely to be significant. The previously reported numerical studies have also highlighted the importance of the modeling of the turbulent dispersion force while simulating solid suspension in a stirred reactor.[11,15,17] Considering these results, the turbulent dispersion of the dispersed phase was considered in the present study. In the present study, the default value of the dispersion Prandtl number, 0.75, was used.

Interphase coupling terms make two-phase flows fundamentally different from single-phase flows. The formulation of time-averaged $\vec{F}_{12,i}$, therefore, must proceed carefully. The interphase momentum exchange term consists of four different interphase

forces: lift force, Basset force, virtual mass force, and drag force.[25] Basset force arises due to the development of a boundary layer around particles and is relevant only for unsteady flows. Basset force involves a history integral, which is time-consuming to evaluate, and in most cases, its magnitude is much smaller than the interphase drag force. The influence of other interphase forces, such as lift force and virtual mass force, on the simulated solid holdup profile was studied by Ljungqvist and Rasmuson.[11] They have found very little influence of the virtual mass and lift force on the simulated solid holdup profiles. Considering this, in the present work, Basset, lift, and virtual mass forces were not considered. The drag force term was only included in the interphase momentum exchange term as

$$\vec{F}_{12,i} = \vec{F}_{D,i} \tag{8}$$

The interphase drag force exerted on phase 2 in the i direction is given by

$$\vec{F}_{D,i} = -\frac{3\alpha_1\alpha_2\rho_1 C_D\left(\sum(U_{2,i} - \vec{U}_{1,i})^2\right)^{0.5}(\vec{U}_{2,i} - \vec{U}_{1,i})}{4d_p} \tag{9}$$

As discussed earlier, the estimation of drag is critical for accurate prediction of a solid concentration distribution. In a solid−liquid stirred reactor, the interphase drag coefficient, C_D, is a complex function of a drag coefficient in a stagnant liquid, C_{D0}, solid holdup present in the reactor, and the prevailing turbulence level. In the present work, we have critically examined the available information to select the appropriate interphase drag formulation.

If the surrounding liquid is turbulent, as in the case of a stirred reactor, the prevailing turbulence is expected to influence the effective drag coefficient on the particles. Experimental measurements of Magelli and co-workers[22,23] and Brucato et al.[20] demonstrate that the prevailing bulk turbulence modifys (increases) the particle drag coefficient to a substantial extent. The magnitude of the effect was found to increase with both particle size and mean turbulent energy dissipation rate. Brucato et al.[20] proposed that the increase in drag coefficient may be related to the ratio of particle size, d_p, to the Kolmogorov length scale, λ, as

$$\frac{C_D - C_{D0}}{C_{D0}} = K\left(\frac{d_p}{\lambda}\right)^3 \tag{10}$$

where C_D is the drag coefficient in turbulent liquid and C_{D0} is the drag coefficient in stagnant liquid.

It should be noted that the flow field around solid particles, which essentially controls interphase drag would be affected not by inertial scale turbulence but by microscale turbulence. It therefore appears logical that the interphase drag coefficient is affected by microscales. Experimental data of Brucato et al.[20] clearly indicates that only microscale turbulence affects the particle drag. The correlation constant K was reported to be 8.67×10^{-4}. It should be noted that the correlation proposed by Brucato et al.[20] was based on their experiments carried out in a Taylor−Couette apparatus. The distribution of energy dissipation rates in the Taylor−Couette apparatus is quite different than that in stirred vessels for the same average energy dissipation rate. This may complicate the direct extension of correlations developed with data collected in the Taylor−Couette apparatus to stirred vessels Recently, Pinelli et al.[22] have measured the settling velocity of the solid particles in a stirred reactor equipped with different multiple impellers and proposed a new correlation (eq 11) relating the decrease in slip velocity with the Kolmogorov length scale of the turbulence, λ.

$$\frac{U_s}{U_t} = 0.4\tanh\left(\frac{16\lambda}{d_p} - 1\right) + 0.6 \tag{11}$$

The comparison of both the correlations (eqs 10 and 11) shows significantly different trends in the observed increase in the particle drag coefficient with an increase in the level of turbulence and the particle size. Also, both these studies have been carried out with very a low volume fraction of solids ($\leq$1%). The solid loading or particle Reynolds number may influence the increase in the drag coefficient due to turbulence. Considering these reported uncertainties in the available knowledge and the difficulties present in the experimentation with higher solid volume fractions motivated us to develop a submodel to understand the influence of the free stream turbulence on the motion of particles having a size in the submillimeter scale with moderately higher solid volume fraction ($5 \leq \alpha < 25\%$).

For gaining a better understanding of the influence of prevailing turbulence on drag coefficient, flow of liquid over a regular array of particles was considered. For reducing demands on computational resources, the flow was modeled in a two-dimensional solution domain using a "unit cell" approach (discussed later in more detail). This means that flow through a bank of regularly arranged cylinders was computationally studied. The influence of the Reynolds number, the volume fraction of solid, and the prevailing turbulence level on the particle drag coefficient was investigated. The standard $k-\epsilon$ turbulence model was used to simulate the turbulence in the flow. The level of prevailing turbulence was varied by specifying different magnitudes of the additional source for turbulence as

$$G = \frac{1}{2}\mu_t(\nabla\vec{U}_i + (\nabla\vec{U}_i)^T)^2 + s \tag{12}$$

where s is the extra source of turbulence. By manipulating the value of such an extra source, volume-averaged values of the effective viscosity, Kolmogorov length scales, and integral time scales of turbulence were varied over a range of interest. The trends observed in the two-dimensional model are expected to be valid for the three-dimensional flow over solid particles. The predicted results on drag coefficients were therefore used to identify an appropriate correlation for estimating interphase drag force on solid particles in turbulent flow. The developed correlation was then evaluated for simulating solid−liquid flow in a stirred reactor by comparing simulated results with the experimental data of Yamazaki et al.[1] and Godfrey and Zhu.[2]

The solid−liquid flow in a stirred reactor was simulated using the multiple reference frame (MRF) approach. Khopkar et al.[26] have recently discussed the formulation of an MRF approach, and hence, it is not discussed here in detail. While implementing the MRF approach, several issues such as the extent and position of the inner region, the number of computational cells, the discretization schemes, the turbulence model, the specific position of the impeller blades, etc. need appropriate selection. The basis for this is discussed below.

2.2. Solution Domain and Boundary Condition. (A) Flow through Regularly Arranged Cylindrical Objects. A unit cell approach was used to model the single-phase flow through regularly arranged cylindrical objects. Cylinders were arranged in a regular square array (see Figure 1). The spacing between the cylinders was calculated by specifying the relevant value of the volume fraction. Figure 1 shows cylindrical objects having a diameter (d_p) equal to 5×10^{-4} m with a volume fraction equal to 15%. The unit cell approach uses the geometrical symmetry to significantly reduce the computational requirements

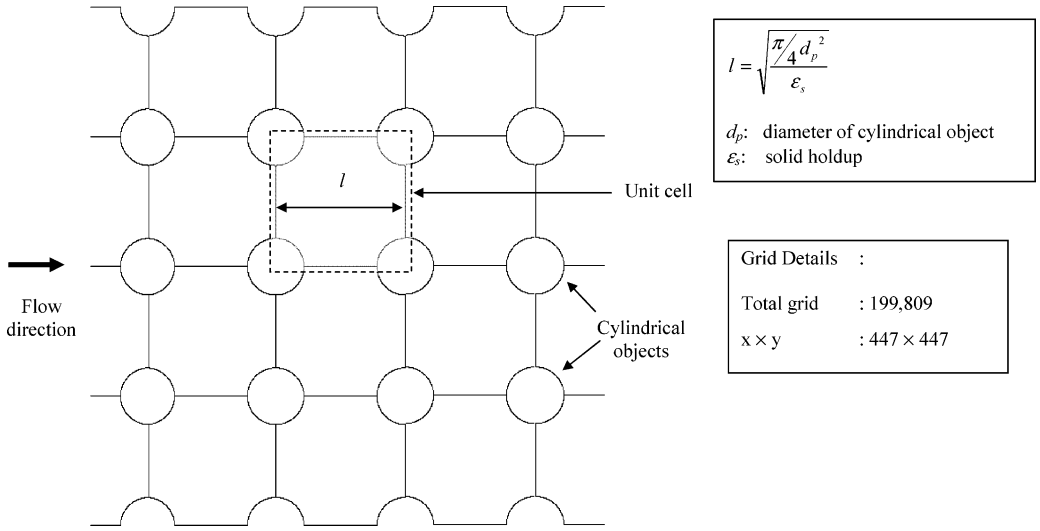

Figure 1. Solution domain for flow through a regular array of cylinders.

(also shown in Figure 1). All the sides of a unit cell were defined as periodic walls. The walls of cylindrical objects were defined with the no-slip boundary condition. Simulations were carried out for different Reynolds numbers (by specifying different values of liquid mass flow rates through the unit cell), volume fractions (by considering different geometries), and levels of prevailing turbulence (by specifying different magnitudes of extra generation, s). The mass flow rate of the liquid was calculated from the terminal settling velocity of the particle as

$$u_\infty = \frac{Re\mu}{\rho d_p} \quad m = \rho u_\infty A_f \tag{13}$$

where A_f is the flow area ($\propto l$, shown in Figure 1) and m is the mass flow rate of the liquid. The direction of the net flow of liquid was set as shown in Figure 1. The simulations were carried out for seven values of particle Reynolds numbers (starting from 0.54 to 69.4) and for four values of the volume fraction of solid (5%, 10%, 15%, and 20%). The turbulent flow around the cylinders was simulated using FLUENT 6.2 (of Fluent Inc., USA). The magnitude of "s" was varied in the range of 0 kg/(s^3 m) to 100 000 kg/(s^3 m) to cover the variation of the Kolmogorov length scale between 1×10^{-4} and 1×10^{-7} m, as usually observed in stirred reactors.

The prediction of flow characteristics especially turbulence quantities is sensitive to the number of grid nodes, grid distribution within the solution domain, and the discretization scheme. In the present work, we used the QUICK (quadratic upstream interpolation for convective kinetics) discretization scheme with a limiter function (SUPERBEE) to avoid nonphysical oscillations. A commercial grid-generation tool, GAMBIT 2.0 (of Fluent Inc., USA) was used to model the geometry and to generate the body-fitted grids. The geometry was modeled with six different grid size distributions with the total number of computational cells ranging from 10 000 to 800 000. The predicted results are discussed in the next section.

(B) Solid−Liquid Stirred Reactor. In the present work, the experimental setups used by Yamazaki et al.[1] and Godfrey and Zhu[2] were considered. All the relevant dimensions such as impeller diameter, impeller off-bottom clearance, reactor height and diameter, and so on were the same as those used by Yamazaki et al.[1] and Godfrey and Zhu.[2] The system investigated consists of a cylindrical, flat-bottomed reactor (of diameter, $T = 0.3$ m [for Yamazaki et al.[1]] and $T = 0.154$ m [for Godfrey and Zhu[2]], and liquid height, $H = T$). Four baffles of width $0.1T$ were mounted perpendicular to the reactor wall. The shaft of the impeller was concentric with the axis of the reactor and extended to the bottom of the reactor. A Rushton turbine (of diameter, $D = 0.1$ m) and a 4-blade down pumping pitched blade (of diameter, $D = 0.052$ m) were used for the setups of Yamazaki et al.[1] and Godfrey and Zhu[2], respectively. The impeller off-bottom clearance was ($C = T/3$) measured from the bottom of the reactor. The physical properties of the liquid and solid particles (spherical glass beads) are given in Table 1.

Table 1. Physical Properties of the Solid−Liquid System

	liquid		solid	
	density (kg/m^3)	viscosity (kg/(m s))	mean particle size (m)	density (kg/m^3)
Yamazaki et al.[1]	1000	1×10^{-3}	135 & 264	2470
Godfrey and Zhu[2]	1096	1.76×10^{-3}	390 & 655	2480

Considering the geometrical symmetry, half of the reactor was considered as a solution domain for the Yamazaki et al.[1] setup and a 90° domain was considered for the Godfrey and Zhu[2] setup (see Figure 2). It is very important to use an adequate number of computational cells while numerically solving the governing equations over the solution domain. The prediction of the turbulence quantities is especially sensitive to the number of grid nodes and the grid distribution within the solution domain. In the present work, the numerical simulations for solid−liquid flows in a stirred reactor were carried out with a grid size of 287 875 ($r \times \theta \times z$: 49 × 93 × 55) for the Yamazaki et al.[1] setup and 275 616 ($r \times \theta \times z$: 58 × 54 × 88) for the Godfrey and Zhu[2] setup. The details of the computational grids used in the present work are shown in Figure 2. In the present work, the QUICK discretization scheme with the SUPERBEE limiter function (to avoid nonphysical oscillations) was used. Standard wall functions were used to specify the wall boundary conditions. The simulated results are discussed in the following section.

3. Results and Discussion

3.1. Flow through Regularly Arranged Cylindrical Objects. Preliminary simulations of flow through regularly arranged cylindrical objects were first carried out for all the six grid size distributions, varied from 10 000 to 800 000 computational cells. On the basis of these numerical simulations, it was found that about 200 000 computational cells were sufficient to capture the key features of the flow (the difference between the predicted

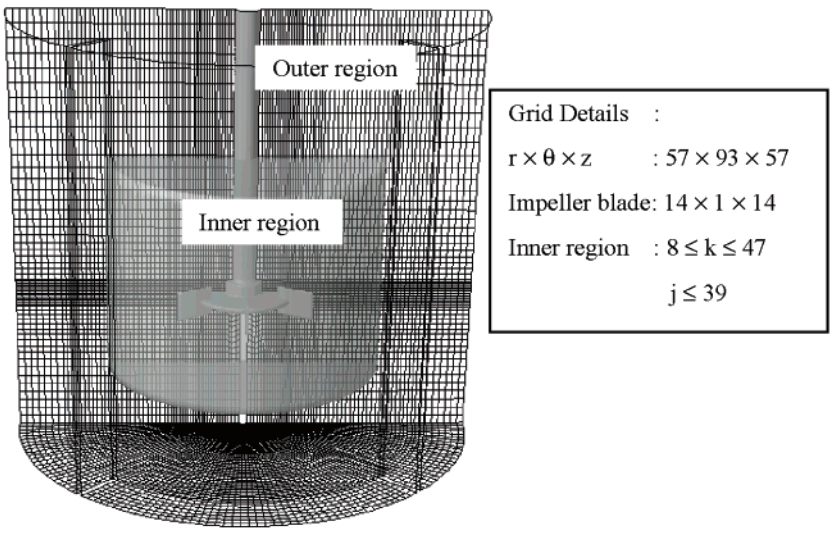

(a) Yamazaki et al.[1] setup

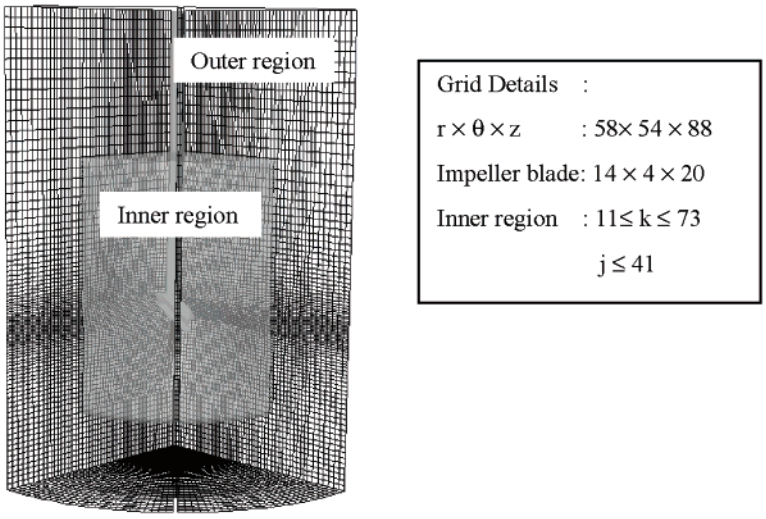

(b) Godfrey and Zhou[2] setup

Figure 2. Computational grid and solution domain of a stirred reactor.

values of pressure drop for 200 000 and 800 000 grid nodes was found to be within 5% of the pressure drop value for 800 000 grid nodes). Therefore, all further simulations were carried out with the grid size of 200 000.

It is essential to validate the computational model before extending its use to understand the influence of free stream turbulence on the particle drag force. This validation was carried out first by comparing predicted drag coefficients with the published[27] numerical and analytical solutions at low Reynolds numbers. The agreement between these results was within 5%. The predicted results at higher Reynolds numbers were then compared with the published correlations of Dybbs and Edwards[28] and Prakash et al.[29] The results predicted in this work were found to lie between the predictions of these two correlations. The validation of the unit cell approach in predicting the influence of solid holdup on the drag coefficient has also been recently published by Gunjal et al.[30] Therefore, the validation results are not included here for the sake of brevity. The computational model was then extended to understand the influence of free stream turbulence on the flow around the particles.

Typical predicted results for the solid volume fraction equal to 15%, a Reynolds number equal to 34.7, and without a source for extra turbulence are shown in Figure 3 in the form of a velocity vector and contour plots. It can be seen from Figure 3 that the computational model has qualitatively predicted the flow field around the cylindrical objects. The predicted velocity field around the cylindrical objects is shown in Figure 3a (i). The predicted velocity field captured the wake behind the cylindrical objects. The predicted pressure and turbulent kinetic energy distribution around the cylindrical objects is shown in Figure 3b (i) and 3c (i). The model has captured the presence of a high pressure and high turbulent kinetic energy region near the nose of the cylindrical objects. Overall, it can be said that the computational model has captured the key details of the flow around cylindrical objects.

An additional source of turbulent kinetic energy was specified using a user-defined function to simulate the presence of extra free stream turbulence in the flowing liquid. The magnitude of this source term was varied to cover the variation of Kolmogorov length scales of turbulence in the range of 1×10^{-5} to 1×10^{-7} m, as usually observed in a stirred reactor. The predicted results show significant increase in pressure drop values with increase in the level of turbulence. The comparison of the predicted results for with and without extra turbulence (Figure 3) shows significant change in the flow field around the

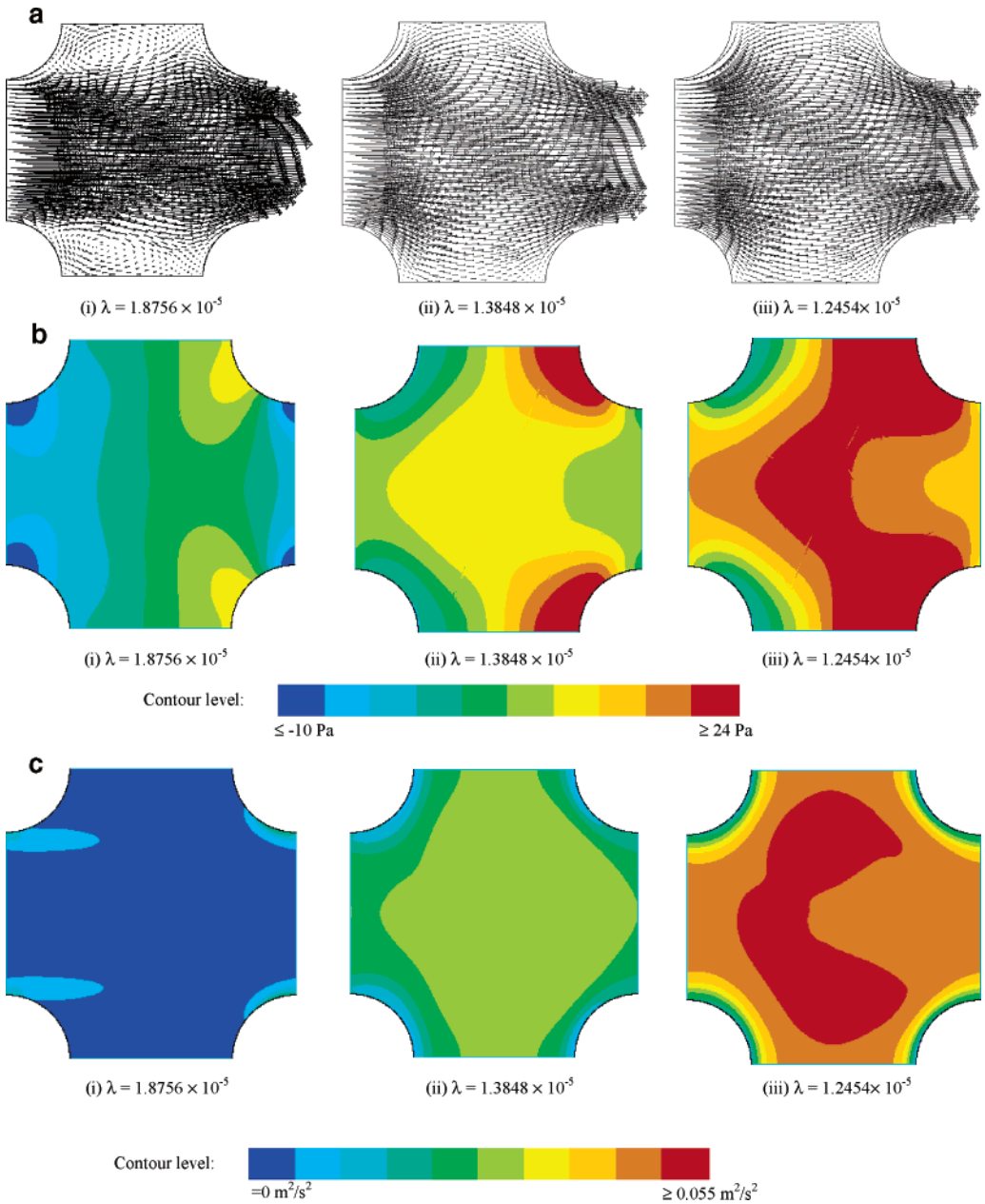

Figure 3. Simulated flow field around the cylindrical objects. (a) Velocity field. (b) Pressure field. (c) Turbulent kinetic energy field.

cylindrical objects. As the level of prevailing turbulence increases, the high pressure region in front of the cylinders increases, resulting in higher form drag. The values of the drag coefficients for these different cases were calculated from the predicted pressure drop (see eq 14).[30] The predicted increase in the drag coefficient with an increase in the prevailing turbulence is consistent with the previously reported experimental studies.[23,31−32]

$$\frac{(\Delta p/L) - (\Delta p/L)_0}{(\Delta p/L)_0} = \frac{C_D - C_{D0}}{C_{D0}} \qquad (14)$$

For a quantitative analysis of the influence of the prevailing turbulence, the approach of Brucato et al.[20] was selected. The results predicted by the CFD model were compared with the available correlations[20,22] in Figure 4. The comparison brings out several salient points. It can be seen from Figure 4 that the predicted values for the lower solid holdup (5%) and for Reynolds number, $Re \leq 34.7$, follow the trends of the correlation of Brucato et al.[20] As the solid holdup increases (≥10%), the predicted values shift toward the right. The computational model has also captured the shift of predicted values toward the right with increase in the particle Reynolds number. This is consistent with the experimental data reported.[20] The predicted results deviate from the trends estimated by correlations of Pinelli et al.[22] for higher ratios of d_p/λ. This correlation was therefore not considered further.

The predicted results clearly indicate that, in addition to d_p/λ, the fractional increase in the drag coefficient is also a function of the particle Reynolds number and the volume fraction. Different alternative approaches have been tried out to incorporate the influence of volume fraction, Reynolds number, and d_p/λ all together to propose a generalized correlation for estimating the increase in the particle drag coefficient in turbulent flow. However, the preliminary analysis indicated difficulty in correlating the data due to limited data points. Considering a rather narrow range of Reynolds numbers relevant to solid−liquid flows in stirred reactors, the influence of

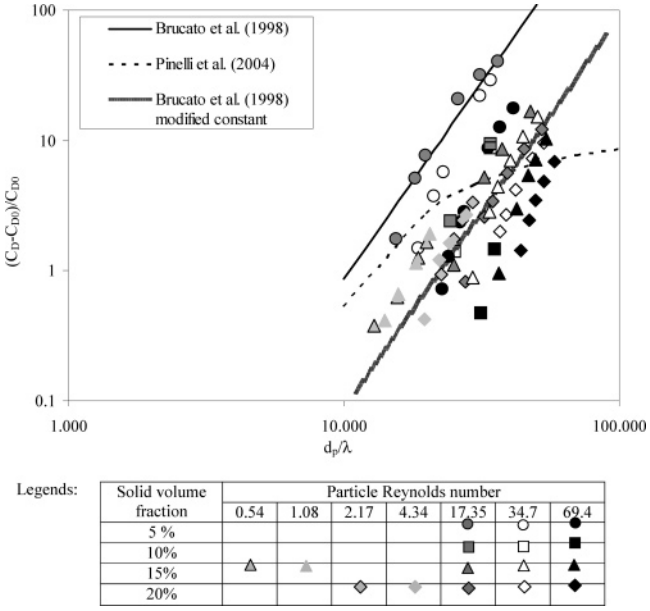

Figure 4. Fractional increase in the particle drag coefficient in turbulent flow.

Reynolds number was ignored in the present study. This obviously has some limitations. These are discussed after comparing the predicted results with the experimental data. Ignoring the possible influence of the solid volume fraction and particle Reynolds number, the predicted results were correlated considering the sole dependence on d_p/λ for a range of solid holdup values ($5 < \alpha < 25\%$). The predicted results however require a proportionality constant 10 times lower and can be correlated (modified correlation of Brucato et al.[20]) as

$$\frac{C_D - C_{D0}}{C_{D0}} = 8.76 \times 10^{-5}\left(\frac{d_p}{\lambda}\right)^3 \qquad (15)$$

where C_D is the drag coefficient in turbulent liquid and C_{D0} is the drag coefficient in the stagnant liquid. The reduction in the proportionality constant in the above equation is discussed later in more detail. Equation 15 (based on volume-averaged properties) was evaluated for estimating effective drag coefficients for solid−liquid flow in a stirred reactor by comparing the simulated results with the experimental data of Yamazaki et al.[1] and Godfrey and Zhu.[2]

3.2. Solid-Liquid Flow in a Stirred Reactor. (A) Interphase Drag Force. The simulation of solid suspension in the stirred reactor was first carried out for a particle size equal to 264 μm ($d_p/\lambda \approx 20$), total solid holdup equal to 10% in the reactor, and an impeller rotational speed equal to 20 rps. The simulations were carried out using both drag coefficient formulations: the drag coefficient formulation proposed by Brucato et al.[20] (eq 10) and the modified Brucato et al.[20] drag coefficient formulation (eq 15). The predicted solid holdup distributions by using both drag coefficient formulations at the midbaffle plane are shown in Figure 5a and b. It can be seen from Figure 5a that, using the Brucato et al.[20] formulation, the computational model has predicted almost a complete suspension of the solid particles. However, the simulated solid holdup distribution using the modified Brucato et al.[20] formulation did not capture the complete suspension of solid particles in the stirred reactor (see Figure 5b). The simulated solid holdup distribution shows the presence of solid accumulation at the bottom and near the axis of the reactor. For quantitative comparison, the predicted solid concentrations/ holdup were compared with the experimental data of Yamazaki et al.[1] The quantitative comparison of the azimuthally averaged axial profile of solid holdup at radial location ($r/T = 0.35$) is shown in Figure 5c. It can be seen from Figure 5c that the computational model with the Brucato et al.[20] drag force formulation overpredicted the solid suspension height. However, the suspension height predicted by the modified correlation was in good agreement with the experimental data.

It will be more instructive to compare the slip velocity distribution predicted by both the correlations to evaluate the difference between the two correlations. The slip velocity distribution at the midbaffle plane predicted using both the correlations is shown in Figure 6. It can be seen from Figure 6

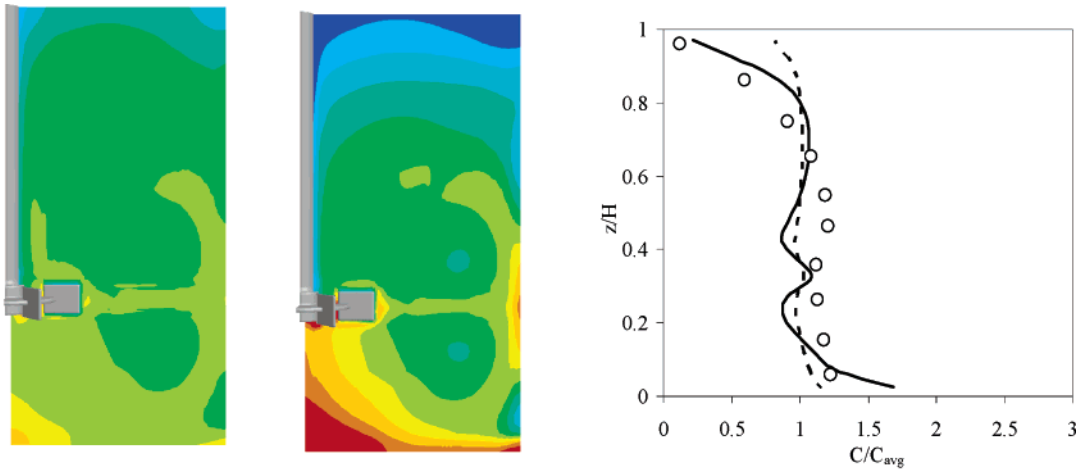

Figure 5. Simulated solid holdup distribution at the midbaffle plane, for $d_p = 264$ μm, $d_p/\lambda \approx 20$, $\alpha = 0.1$, $N = 20.0$ rps, and $U_{tip} = 6.283$ m/s.

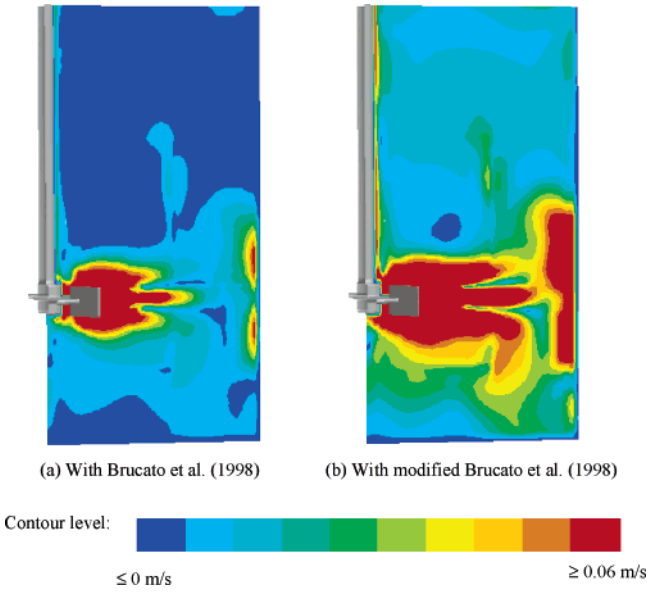

Figure 6. Predicted slip velocity distribution at the midbaffle plane, for d_p = 264 μm, $d_p/\lambda \approx 20$, $\alpha = 0.1$, $N = 20$ rps, and $U_{tip} = 6.283$ m/s.

that higher values of slip velocities are observed in the impeller swept volume, impeller discharge stream, and just above and below the impeller discharge stream near the vessel wall. However, nearly constant values of slip velocities were observed in the upper circulation loop. The comparison of slip velocity distribution for both the correlations indicated that the higher values of the slip velocity were predicted with the modified Brucato et al.[20] correlation. It can be seen that the predicted volume-averaged value of the slip velocity using the modified Brucato et al.[20] correlation (4.1×10^{-2} m/s) was almost 3 times higher than the slip velocity value predicted by using the Brucato et al.[20] correlation (1.39×10^{-2} m/s).

(B) Effect of Particle Size. The particle size is one of the important parameters, and it controls the increase in the particle drag coefficient due to turbulence. The computational model was used to understand the influence of the particle diameter. The simulations of solid suspension in the stirred reactor were then carried out for three more particle sizes, viz., 135 μm (with a Rushton turbine, impeller rotational speed equal to 15 rps, $d_p/\lambda \approx 9$, and $\alpha = 0.15$), 390 μm (with a down pumping pitched turbine, impeller rotational speed equal to 20 rps, $d_p/\lambda \approx 33$, and $\alpha = 0.12$), and 655 μm (with a down pumping pitched turbine, impeller rotational speed equal to 26.7 rps, $d_p/\lambda \approx 60$, and $\alpha = 0.12$).

The predicted solid holdup distribution obtained with both the drag coefficients with volume-averaged values of Kolmogorov scale of turbulence for 135 μm particles ($d_p/\lambda \approx 9$) are shown in Figure 7a and b. It can be seen from Figure 7a and b that the solid holdup distribution predicted by using the modified correlation (eq 15) shows the presence of more solids at the bottom of the reactor compared to the solid holdup distribution predicted by using the Brucato et al.[20] drag coefficient formulation. The quantitative comparison of the azimuthally averaged axial profile of solid holdup at radial location ($r/T = 0.35$) is shown in Figure 7c. It can be seen from Figure 7c that the computational model with both the formulations reasonably predicted the solid holdup distribution and shows a relatively small influence of the drag coefficient formulation on the predicted results.

The computational model was then used to simulate the solid suspension in a stirred reactor equipped with a 4-blade down pumping pitched turbine for two particle sizes 390 μm ($d_p/\lambda \approx$ 33) and 655 μm ($d_p/\lambda \approx 60$), respectively, for $\alpha = 0.12$. The predicted solid holdup distributions with both drag coefficient formulations for 390 μm as well as 655 μm size particles are shown in Figures 8 and 9, respectively. It can be seen from Figures 8 and 9 that, similar to the 264 μm particle, the modified Brucato et al.[20] drag coefficient formulation predicted the suspension quality in the stirred reactor reasonably well. However, the drag coefficient formulation proposed by Brucato et al.[20] has overpredicted the suspension quality and the extent of overprediction has found to increase with an increase in the particle size or the d_p/λ ratio. These figures clearly demonstrate the need for modifying the proportionality constant appearing

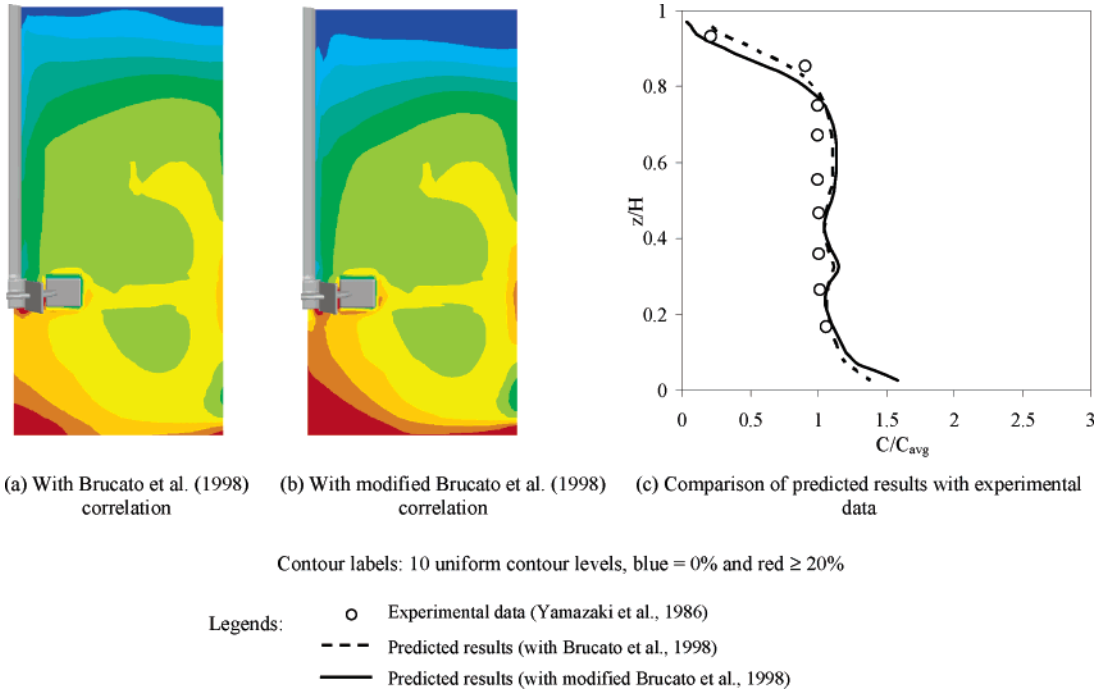

Figure 7. Simulated solid holdup distribution at the midbaffle plane, for d_p = 135 μm, $d_p/\lambda \approx 9$, $\propto = 0.15$, $N = 15.0$ rps, and $U_{tip} = 4.7124$ m/s.

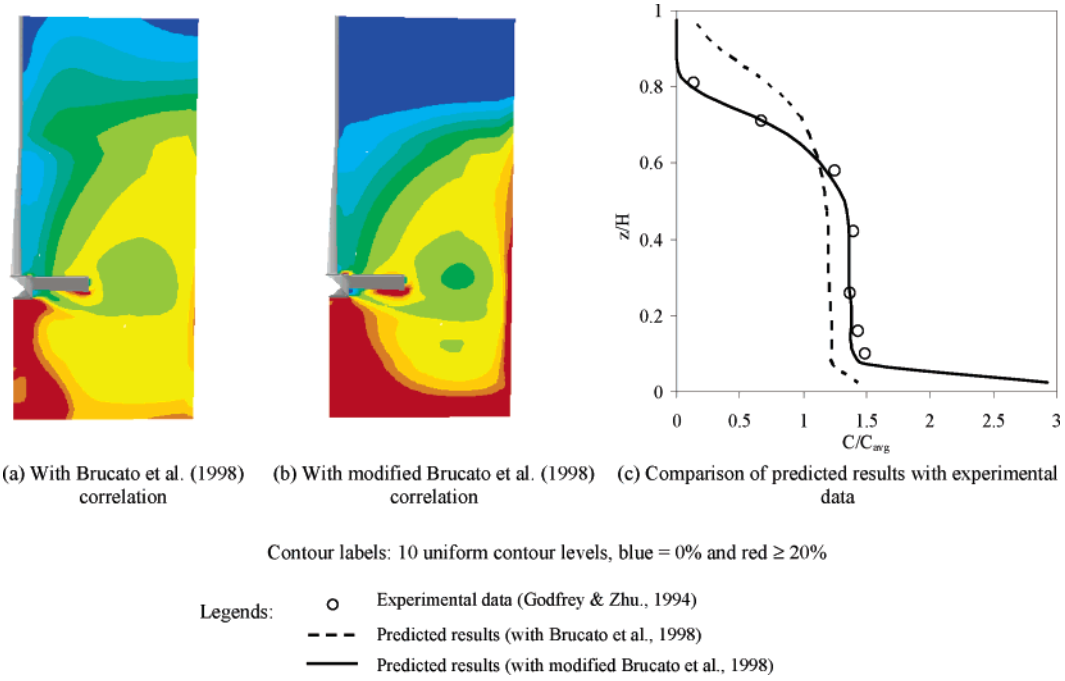

Figure 8. Simulated solid holdup distribution at the midbaffle plane, for $d_p = 390\ \mu$m, $d_p/\lambda \approx 35$, $\alpha = 0.12$, $N = 20.0$ rps, and $U_{tip} = 3.27$ m/s.

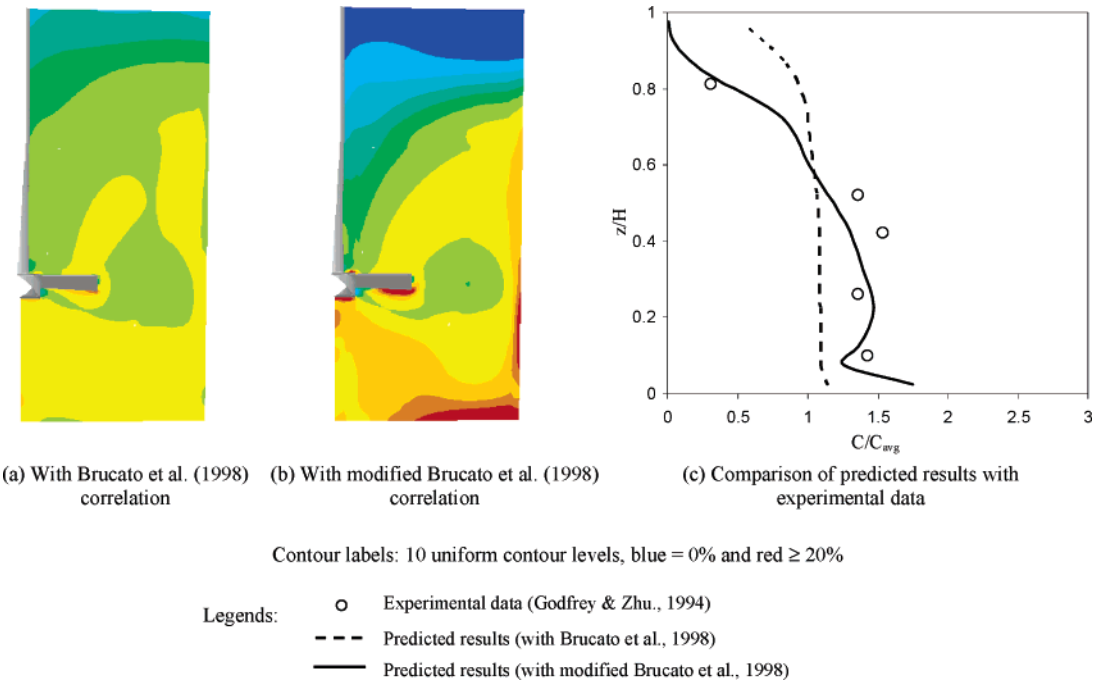

Figure 9. Simulated solid holdup distribution at the midbaffle plane, for $d_p = 655\ \mu$m, $d_p/\lambda \approx 63$, $\alpha = 0.12$, $N = 26.7$ rps, and $U_{tip} = 4.36$ m/s.

in the correlation of Brucato et al.[20] The original experimental data used for formulating the correlation of Brucato et al.[20] indicates the trend of reduction in the proportionality constant as the particle size increases. Recently, Khopkar and Ranade[33] have shown via their simulations of gas−liquid flow in a stirred reactor that for 4 mm particles the proportionality constant in eq 15 had to be reduced to 6.5×10^{-6} (~100 times less than that reported by Brucato et al.[20]). The simulations of solid−liquid suspension in stirred vessels carried out in this work indicate that the modified correlation (shown in eq 15) is able to represent the suspension of solid particles up to 655 μm.

The critical analysis of all the 2D (flow over an array of cylinders) and 3D (solid suspension in stirred vessels) simulations however indicate that the proportionality constant is not solely determined by the particle size. It may also be affected by solid holdup. To examine this, the developed computational model was used to simulate the solid suspension with higher solid holdup for $d_p = 655\ \mu$m (in the experimental setup of Godfrey and Zhu[2] with solid holdup, $\alpha = 0.16$; the value of d_p/λ for this case was about 63). The predicted solid holdup distributions are compared with the experimental data in Figure 10. It can be seen from Figure 10 that both the drag models have overpredicted the suspension quality. Despite the overprediction, the modified Brucato et al.[20] correlation was able to predict the presence of a clear liquid layer ($H_{susp} = 0.83H$) as observed in the experiments ($H_{susp} = 0.68H$), whereas the Brucato et al.[20] correlation, however, predicted a complete suspension of the solids.

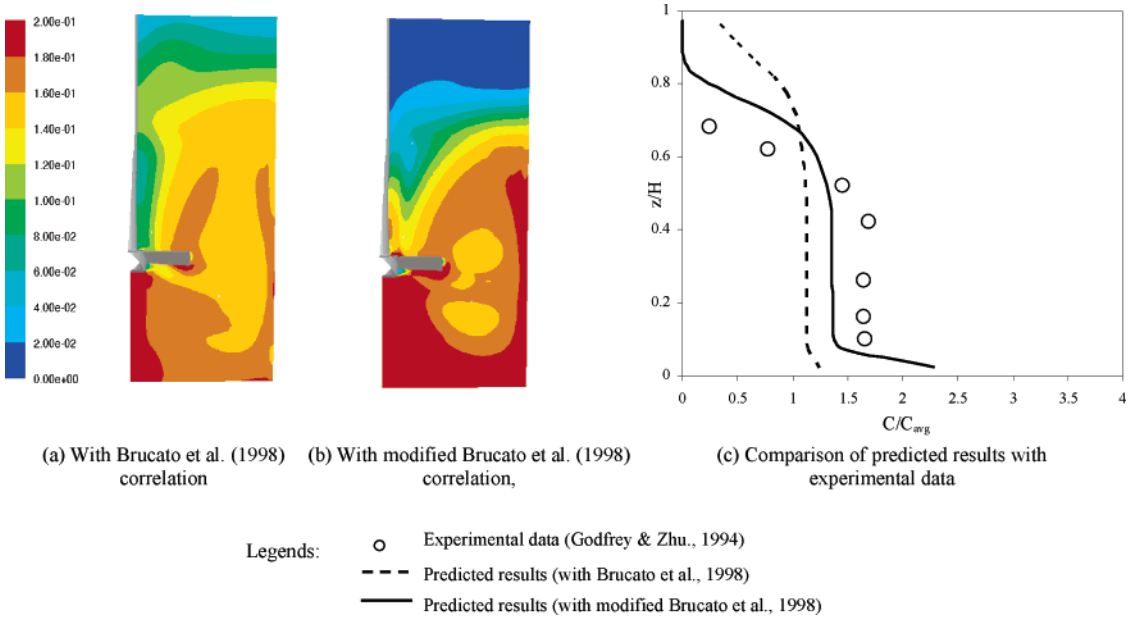

Figure 10. Simulated solid holdup distribution, for $d_p = 655$ μm, $\alpha = 0.16$, $d_p/\lambda = 60$, $N = 20$ rps, and $U_{tip} = 3.267$ m/s.

These results clearly indicate the need for further research on understanding the influence of solid holdup and particle size on the effective drag coefficient. The approach and models presented here will be useful for such further work. In its present form, the model presented here is useful to simulate dense slurry reactors with solid holdup of less than 16% and with particle diameters up to 655 μm. This is a fairly general range and covers most of the industrially relevant slurry reactors. The computational model was then used to estimate the critical impeller speed required for just off-bottom suspension.

(C) Critical Impeller Speed. The concept of the critical impeller speed for just off-bottom suspension (N_{js}) and critical impeller speed for just complete suspension (N_s) were introduced more than forty years ago[34] and are primary design parameters used today by engineers for scale-up and design of stirred slurry reactors. The developed computational model was further extended to estimate both the critical impeller speeds. Different criteria are available to evaluate the N_{js}. However, it is rather difficult to obtain a unique value of N_{js} from all these criteria. The more widely used criteria proposed by Zwietering[34] identifies the N_{js} as a minimum speed required for suspending the solid particles from the bottom of the reactor. It also says that at N_{js} particles may not spend more than 1−2 s at the bottom of the reactor. Kee and Tan[35] have proposed a method to estimate the critical suspension speed from numerical simulations. They have suggested to use the critical impeller speed at which the particles attain positive velocities. In the Eulerian−Eulerian approach as used in this work, it is difficult to use Zwietering's[34] criterion. Instead of using the method of Kee and Tan,[35] in this work, we preferred the method proposed by Bohnet and Niesmak[36] which is based on a standard deviation which is more suitable for steady-state simulations. Bohnet and Niesmak[36] quantify the suspension quality in the reactor using the standard deviation defined as

$$\sigma = \sqrt{\frac{1}{n}\sum_{i=1}^{n}\left(\frac{\alpha_{2i}}{\alpha_{2,avg}} - 1\right)^2} \qquad (16)$$

where n is the number of sampling locations used for measuring the solid volume fraction. The increase in the degree of homogenization (better suspension quality) is manifested as the reduction of the standard deviation value. On the basis of the quality of the suspension, the range of the standard deviation is broadly divided into three ranges. For uniform (homogeneous) suspensions, the value of the standard deviation is found to be smaller than 0.2 ($\sigma < 0.2$). However, for the just suspension condition, the value of the standard deviation lies between 0.2 and 0.8 ($0.2 < \sigma < 0.8$), and for an incomplete suspension, $\sigma > 0.8$.[18]

The simulations of suspensions of solid particles (with a size 264 μm and solid holdup of 10%) in a stirred reactor were carried out using the modified drag coefficient formulation for nine impeller rotational speeds (starting from 2 to 25 rps). The values of the standard deviation were then calculated using eq 16. In the present study, the standard deviation was calculated using the values of the solid volume fraction stored at all computational cells. The variation of the standard deviation values with respect to the impeller rotational speed is shown in Figure 10. The computational model has predicted the sharp reduction in the standard deviation values as the impeller speed approaches the critical impeller speed required for a just off-bottom suspension. It can be seen from Figure 10 that the impeller speed required to achieve the just off-bottom suspension lies between 13 and 15 rps, which is in good agreement with the critical impeller speed (13.4 rps) estimated using the correlation proposed by Zwietering.[34] With further increase in the impeller speed, the value of the standard deviation decreases rather slowly. It can be seen from Figure 10 that, even with an impeller rotational speed of 25 rps, the system did not achieve a homogeneous suspension ($\sigma = 0.34$). However, the computational model with the drag coefficient fomulation of Brucato et al.[20] overpredicted the suspension quality (for the impeller speed of 13.4 rps, the predicted $\sigma = 0.253$).

The computational model was further used to understand the influence of impeller rotational speed on the predicted solid holdup distribution near the reactor bottom. The predicted solid holdup distribution at a height of 0.005 m from the reactor bottom is shown in Figure 11. It can be seen from Figure 11 that, for an impeller rotational speed of 2 rps, the predicted solid holdup distribution shows the presence of all the solids at the bottom of the reactor, indicating the inability of the impeller

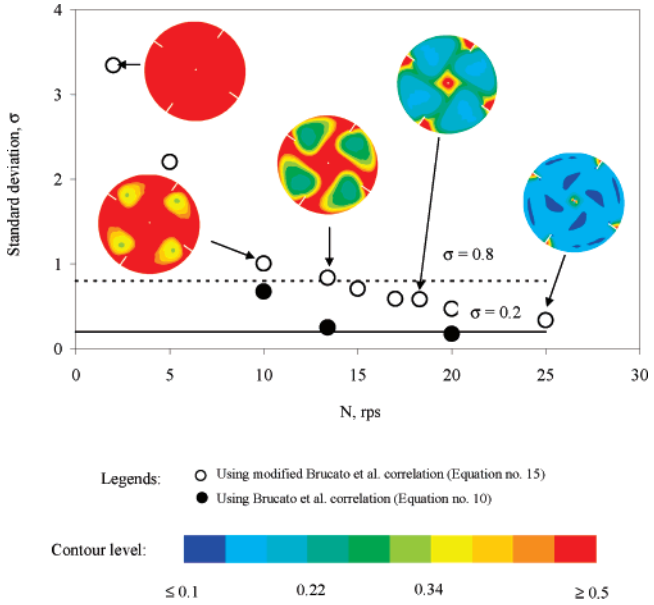

Figure 11. Predicted influence of the impeller rotational speed on suspension quality for $d_p = 264$ μm and $\alpha = 0.1$.

action to suspend the solids in the bulk volume of the reactor. The further increase in the impeller speed leads to an increase in the amount of solids suspended in the bulk volume of the reactor. However, the impeller action was still found to be unable to suspend the solids from the bottom of the reactor. It can be seen from Figure 11 that a minimum impeller rotational speed of 10 rps is required to just move the solids from the bottom layer. The predicted solid holdup distribution for an impeller rotational speed of 13.4 rps is shown in Figure 11. It can be seen that the impeller action is now sufficient to move the solids from the bottom of the impeller, and it can be said that the system is close to the just off-bottom suspension condition. Similarly, the predicted solid holdup distribution at the bottom of the reactor for impeller rotational speeds equal to 18.3 and 25 rps are shown in Figure 11. It can be see from Figure 11 that with further increase in the impeller rotational speed the amount of solid particles present at the bottom of the reactor has decreased. It is also seen from Figure 11 that, for an impeller rotational speed equal to 25 rps, the predicted results show a nearly uniform solid holdup distribution at the bottom of the reactor, indicating that the system is close to the just homogeneous suspension condition.

It is, however, difficult to exactly identify the critical impeller speed required to achieve the just complete suspension from the values of the standard deviation. Kraume[37] used the criteria of cloud height to identify the critical impeller speed required for a complete suspension ($H_{cloud} = 0.9H$). The predicted cloud height for four impeller rotational speeds (10, 13.4, 18.3, and 25 rps) is shown in Figure 12. The computational model has captured the increase in the cloud height with an increase in the impeller rotational speed. Similar observations have been reported by Micale et al.[38] It can be seen from Figure 12 that the impeller rotational speed required to achieve the just complete suspension is $N_s = 18.3$ rps ($H_{cloud} = 0.91H$ for 18.3 rps), which is in good agreement with the experimental observations (18.3 rps) of Yamazaki et al.[1]

Kraume[37] has also observed very low values of liquid velocities in the clear liquid layer. The predicted results were then further checked to understand the influence of the presence of solids on the liquid-phase velocities. The predicted values of the liquid-phase velocity magnitudes were compared with

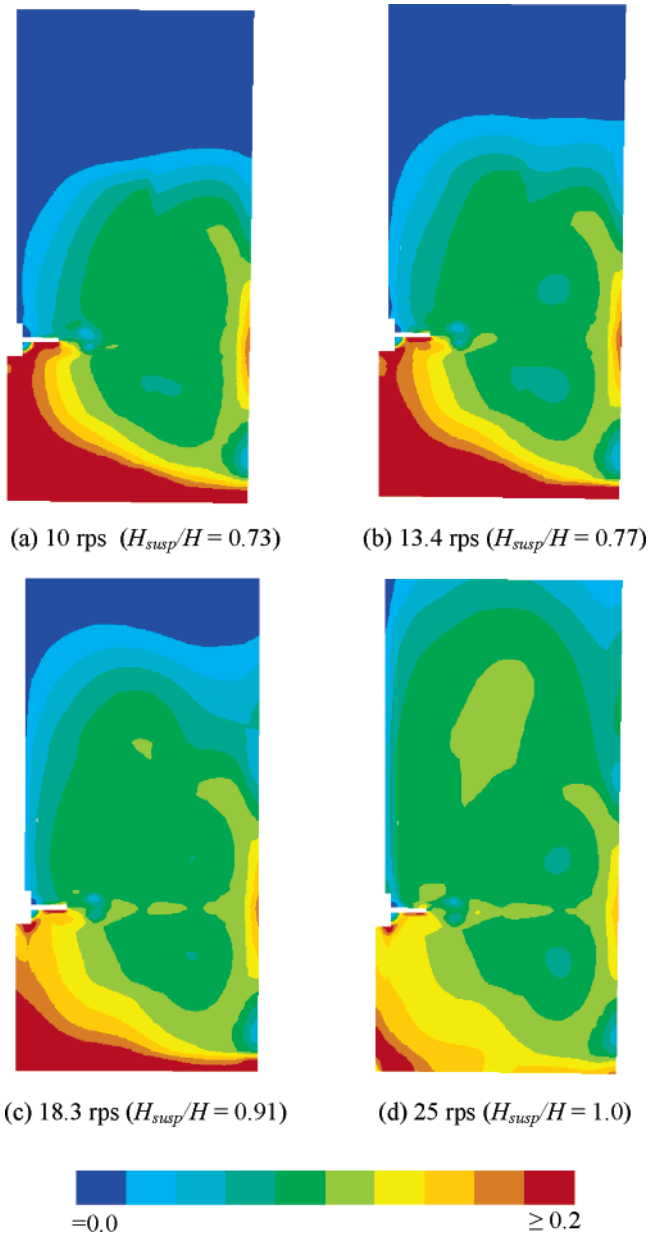

Figure 12. Predicted suspension height for four different impeller rotational speeds for $d_p = 264$ μm and $\alpha = 0.1$.

the single-phase results at an axial height of 0.28 m from the bottom of the reactor. The comparison of the liquid-phase velocity magnitudes is shown in Figure 13. It can be seen from Figure 13 that the computational model has predicted a significant reduction in liquid velocity values for solid−liquid flows near the top surface as observed in the experiments. It is important to capture such reduction in the liquid-phase velocities which may have important implications for mixing in solid−liquid systems.

4. Conclusions

The preliminary simulations of a dense stirred slurry reactor highlighted the importance of correct modeling of the interphase drag force. A CFD based two-dimensional model problem was then developed to understand the influence of prevailing turbulence and the presence of neighboring particles on the particle drag coefficient. The two-fluid model along with the standard $k-\epsilon$ model of turbulence with mixture properties was then developed to simulate solid−liquid flows. The model was

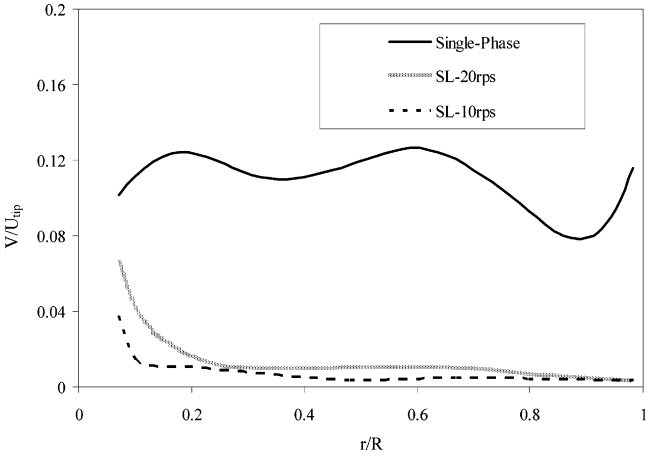

Figure 13. Comparison of normalized liquid-phase velocity magnitudes near the top surface, for $d_p = 264\ \mu$m, $d_p/\lambda \approx 20$, and $\alpha = 0.1$.

used to simulate solid suspension in a stirred reactor. The predicted results were compared with the experimental data of Yamazaki et al.[1] and Godfrey and Zhu.[2] The computational model was then used to understand the influence of the particle size on the performance of the model. The model was also used to estimate the critical impeller speed required for a just off-bottom suspension as well as a just complete suspension. The key conclusions based on this study are listed in the following.

(1) A unit cell approach was useful in understanding the influence of the prevailing turbulence, solid volume fraction, and Reynolds number on the effective drag coefficient. The influence of prevailing turbulence on the drag coefficient can be estimated by the correlation of Brucato et al.[20] The results obtained from the two-dimensional model showed that, for higher solid loading and larger particle Reynolds numbers, the proportionality constant appearing in the correlation of Brucato et al.[20] needs to be reduced. This trend was found to be consistent with the results reported by Khopkar and Ranade.[33]

(2) A 10 times lower value of the proportionality constant ($K = 8.76 \times 10^{-5}$) as used in this work was found to be useful to simulate solid suspension in stirred vessels when solid holdup is less than 16% and particle size is less than 655 μm. Further work is needed to delineate influences the particle Reynolds number, solid volume fraction, and ratio of particle diameter to Kolmogorov's length scale on the effective drag coefficient.

(3) The computational model with the modified Brucato et al.[20] correlation reasonably predicted the value of the critical impeller speed required for a just off-bottom suspension (N_{js}) and the critical impeller speed required for a just complete suspension (N_S).

(4) The computational model with modified Brucato et al.[20] has reasonably predicted the suspension quality and also captured the significant reduction in the liquid velocities in the top clear liquid layer as observed in the experiments.[34]

Despite some deficiencies, the computational model developed in the present study shows promising results and seems to be able to predict the solid suspension in a dense stirred slurry reactor. The model and results presented in this paper would be useful for extending the application of CFD based models for understanding the influence of suspension quality on the liquid-phase mixing process and for simulating large stirred slurry reactors.

Acknowledgment

One of the authors (A.R.K.) is grateful to CSIR for providing a research fellowship. One of the authors (G.R.K.) is grateful to UGC for providing a research fellowship. A Department of Science and Technology Grant (No. DST/SF/40/99) supported part of the work. The authors are grateful to Professor J. C. Godfrey, Department of Chemical Engineering, University of Bradford, UK, for providing the experimental data.

Notations

A_f = flow area, m^2
C = impeller off-bottom clearance, m
C_D = drag coefficient in turbulent liquid
C_{D0} = drag coefficient in still liquid
C_{lift} = lift coefficient
D_i = impeller diameter, m
D_{12} = turbulent diffusivity, m^2/s
d_p = particle diameter, m
f = friction factor
F_D = interphase drag force, N/m^3
F_{lift} = interphase lift force, N/m^3
G = turbulence generation, (kg m)/s^3
g = acceleration due to gravity, m/s^2
H = reactor height, m
H_{cloud} = cloud height, m
k = turbulent kinetic energy, m^2/s^2
N = impeller rotational speed, rps
m = mass flow rate, kg/s
Re_p = particle Reynolds number
p = pressure, N/m^2
r = radial coordinate, m
s = extra source of turbulence, kg/(m s^3)
S_ϕ = source term for ϕ
T = reactor diameter, m
t = time, s
U = velocity, m/s
U_s = slip velocity, m/s
U_t = terminal settling velocity of particle, m/s
U_{tip} = impeller tip speed, m/s
V = volume of reactor, m^3
w = impeller blade height, m
x = position vector, m
z = axial coordinate, m

Greek Letters

α = volume fraction
ϵ = turbulent kinetic energy dissipation rate, m^2/s^3
λ = Kolmogorov length scale, m
ρ = density, kg/m^3
μ = viscosity, kg/(m s)
τ = shear stress, N/m^2
σ = standard deviation

Subscripts

1 = liquid
2 = solid
q = phase number
t = turbulent

Literature Cited

(1) Yamazaki, H.; Tojo, K.; Miyanami, K. Concentration profiles of solids suspended in a stirred tank. *Powder Technol.* **1986**, *48*, 205.

(2) Godfrey, J. C.; Zhu, Z. M. Measurement of particle liquid profiles in agitated tanks. *AIChE Symp. Ser.* **1994**, *299*, 181.

(3) Ranade, V. V. *Computational Flow Modelling for Chemical Reactor Engineering*; Academic Press: New York, 2002.

(4) Myers, K. J.; Bakker, A.; Fasano, J. B. Simulation and experimental verification of liquid−solid agitation performance. *AIChE Symp. Ser.* **1995**, *305* (91), 139.

(5) Brucato, A.; Ciofalo, M.; Godfrey, J.; Grisafi, F.; Micale, G. Experimental and CFD simulation of solids distribution in stirred reactors. *Proceedings of the 5th International Conferernce on Multiphase Flow in Industrial Plants*; Amalfi, Italy, 1996; p 323.

(6) Brucato, A.; Ciofalo, M.; Grisafi, F.; Magelli, F.; Torretta, F. On the simulation of solid particle distribution in multiple impeller agitated tanks via computational fluid dynamics. *Proceedings of ECCE 1*, Florence, Italy, 1997; p 1723.

(7) Decker, S.; Sommerfeld, M. Calculation of particle suspension in agitated reactors with the Euler−Lagrange approach. *Inst. Chem. Eng. Symp. Ser.* **1996**, *140*, 71.

(8) Barrue, H.; Xureb, C.; Bertrand, J. A computational study on solid suspension in stirred reactor. *Proceedings of ECCE 1,* Florence, Italy, 1997; p 1843.

(9) Gosman, A. D.; Lekakou, C.; Politis, S.; Issa, R. I.; Looney, M. K. Multidimensional modeling of turbulent two-phase flows in stirred reactors. *AIChE J.* **1992**, *38* (12), 1947.

(10) Micale, G.; Montante, G.; Grisafi, F.; Brucato, A.; Godfrey, J. CFD simulation of particle distribution in stirred reactors. *Trans. Inst. Chem. Eng*., *Part A* **2000**, *78*, 435.

(11) Ljungqvist, M.; Rasmuson, A. Numerical simulation of the two-phase flow in an axially stirred reactor. *Trans. Inst. Chem. Eng*., *Part A* **2001**, *79*, 533.

(12) Altway, A.; Setyavan, H. M.; Winardi, S. Effect of particle size on the simulation of three-dimensional solid dispersion in stirred tanks. *Trans. Inst. Chem. Eng.* **2001**, *79*, 1011.

(13) Sha, Z.; Palosarri, S.; Oinas, P.; Ogawa, K. CFD simulation of solid suspension in a stirred tank. *J. Chem. Eng. Jpn.* **2001**, *34* (5), 626.

(14) Wang, F.; Wang, W.; Wang, Y.; Mao, Z. S. CFD simulation of solid−liquid two phase flow in baffled stirred reactors with Rushton impellers. *Proceedings of the 3rd International Conference on CFD in the Minerals and Process Industry*; Melbourne, Australia, 2003; p 287.

(15) Angst, R.; Harnack, E.; Singh, M.; Kraume, M. Grid and model dependency of the solid/liquid two-phase flow CFD simulation of stirred reactors. *Proceedings of* the *11th European Conference of Mixing*; Bamberg, Germany, 2003; p 347.

(16) Derksen, J. J. Numerical Simulation of solid suspension in a stirred tank. *AIChE J*. **2003**, *49*, 2700.

(17) Barrue, H.; Bertrand, J.; Cristol, B.; Xuereb, C. Eulerian Simulation of Dense Solid−Liquid Suspension in Multi-Stage Stirred Reactor. *J. Chem. Eng. Jpn.* **2001**, *34* (5), 585.

(18) Oshinowo, L. M.; Bakker, A. CFD modeling of solids suspensions in stirred tanks. *Symposium on Computational Modeling of Metals, Minerals and Materials*, TMS Annual Meeting, Seattle, WA, 2002.

(19) Ranade, V. V.; Tayaliya, Y. Computational study of transfer and dissipation of impeller power. Presented at ISHMT-15 Conference, Pune, India, 2000.

(20) Brucato, A.; Grisafi, F.; Montante, G. Particle drag coefficients in turbulent fluids. *Chem. Eng. Sci.* **1998**, *53* (18), 3295.

(21) Montante, G.; Micale, G.; Magelli, F.; Brucato, A. Experiments and CFD prediction of solid particle distribution in a reactor agitated with four pitched blade turbines. *Trans. Inst. Chem. Eng., Part A* **2001**, *79*, 1005.

(22) Pinelli, D.; Montante, G.; Magelli, F. Dispersion coefficient and settling velocities of solids in slurry reactors stirred with different types of multiple impellers. *Chem. Eng. Sci.* **2004**, *59*, 3081.

(23) Magelli, F.; Fajner, D.; Nocentini, M.; Pasquali, G. Solid distribution in reactors stirred with multiple impellers. *Chem. Eng. Sci.* **1990**, *45* (3), 615.

(24) Montante, G.; Magelli, F. Modelling of solids distribution in stirred tanks: Analysis of simulation strategies and comparison with experimental data. *Int. J. Comput. Fluid Dyn.* **2005**, *19*, 253.

(25) Ranade, V. V. Numerical simulation of dispersed gas−liquid flows. *Sadhana* **1992**, *17*, 237.

(26) Khopkar, A. R.; Mavros, P.; Ranade, V. V.; Bertrand, J. Simulation of flow generated by an axial flow impeller: Batch and continuous operation. *Chem. Eng. Res. Des.* **2004**, *82* (A6), 737.

(27) Satheesh, V, K.; Chhabra, R. P.; Eswaran, V. Steady incompressible fluid flow over a bundle of cylinders at moderate Reyonods number. *Can. J. Chem. Eng*. **1999**, *77*, 978.

(28) Dybbs, A.; Edwards, R. V. A new look at porous media fluid mechanics, Darcy to turbulent. In *Fundamentals of transport phenomena in porous media*; Bear, J., Carapcioglu, Y., Eds.; Martinus Nijhoof: The Hague, 1984; p 199.

(29) Prakash, O.; Gupta, S. N.; Mishra, P. Newtonian and inelastic non-Newtonian flow across tube banks. *Ind. Eng. Chem. Res.* **1987**, *26*, 1365.

(30) Gunjal, P. R.; Ranade, V. V.; Chaudhari, R. V. Computational study of a single-phase flow in packed beds of sphere. *AIChE J.* **2005**, *51* (2), 365.

(31) Uhleherr, P. H. T.; Sinclair, C. G. The effect of free stream turbulence on the drag coefficient of spheres. *Proceedings Chemeca*; Butterworths: Melbourne, 1970; p 70.

(32) Clift, R.; Gauvin, W. H. Motion of entrained particles in gas streams. *Can. J. Chem. Eng.* **1971**, *49*, 439.

(33) Khopkar, A. R.; Ranade, V. V. CFD simulation of gas−liquid stirred vessel: VC, S33 and L33 flow regimes. *AIChE J*. **2006**, *52* (5), 1654.

(34) Zwietering, T. N. Suspending of solid particles in liquid by agitation. *Chem. Eng. Sci.* **1958**, *8*, 244.

(35) Kee, N. C. S.; Tan, R. B. H. CFD simulation of solids suspension in mixing vessels. *Can. J. Chem. Eng*. **2002**, *80*, 721.

(36) Bohnet, M.; Niesmak, G. Distribution of solids in stirred suspension. *Ger. Chem. Eng.* **1980**, *3*, 57.

(37) Kraume, M. Mixing times in stirred suspension. *Chem. Eng. Technol.* **1992**, *15*, 313.

(38) Micale, G.; Girsafi, F.; Rizzuti, L.; Brucato, A. CFD simulation of particle suspension height in stirred vessels. *Chem. Eng. Res. Des*. **2004**, *82*, 1204.

Received for review August 16, 2005
Revised manuscript received February 26, 2006
Accepted April 13, 2006

IE050941Q